

gering is markedly reduced at neutron number 75.

We thank Professor H. Walther and Dr. W. Hartig, then at the University of Cologne, who introduced us into the art of handling dye lasers. We are also indebted to Professor E.-W. Otten and Dr. R. Neugart of Mainz University for many stimulating discussions and advice.

¹C. Duke, H. Fischer, H.-J. Kluge, H. Kremmling, Th. Köhl, and E. W. Otten, *Phys. Lett.* **60A**, 303 (1977).

²R. Neumann, F. Träger, J. Kowalski, and G. zu Putlitz, *Z. Phys.* **A279**, 249 (1976).

³W. Hartig and H. Walther, *Appl. Phys.* **1**, 171 (1973);

H. Hartwig, Diplomarbeit, Cologne University, 1973 (unpublished).

⁴H. Fabricius, K. Freitag, and S. Göring, *Nucl. Instrum. Methods* **38**, 64 (1965); H. Fabricius, K. Freitag, S. Göring, A. Hanser, and H.-J. Langmann, *Kernforschungszentrum Karlsruhe Report No. KFK-511*, 1966 (unpublished).

⁵D. von Ehrenstein, G. C. Morrison, J. A. Nolen, Jr., and N. Williams, *Phys. Rev. C* **1**, 2066 (1970).

⁶H.-J. Kluge and H. Sautter, *Z. Phys.* **270**, 295 (1974); M. W. Swagel and A. Lurio, *Phys. Rev.* **169**, 114 (1969).

⁷L. Olschewski and E.-W. Otten, *Z. Phys.* **196**, 77 (1966).

⁸W. Fischer, M. Hartmann, H. Hühnermann, and H. Vogt, *Z. Phys.* **267**, 209 (1974).

⁹C. Höhle, H. Hühnermann, Th. Meier, H. R. Ihle, and R. Wagner, *Phys. Lett.* **62B**, 390 (1976).

Measurement of Spin-Exchange Effects in Electron-Hydrogen Collisions: Impact Ionization

M. J. Alguard, V. W. Hughes, M. S. Lubell, and P. F. Wainwright

J. W. Gibbs Laboratory, Yale University, New Haven, Connecticut 06520

(Received 29 June 1977)

We have measured the interference between the direct and exchange scattering amplitudes in electron impact ionization of atomic hydrogen over the energy range 15 to 197 eV in a crossed-beams experiment utilizing spin-polarized electrons and spin-polarized hydrogen atoms. The experimental values for the asymmetry $A = (\sigma^{**} - \sigma^{**}) / (\sigma^{**} + \sigma^{**})$ in the total ionization cross section for antiparallel and parallel incident- and atomic-electron spins are inconsistent with all theoretical calculations below 50 eV.

Although the electron-hydrogen collision problem is the most fundamental of all electron-atom collision problems, the mathematical description of the process cannot be carried out in closed form because a solution to a three-body problem is required. The situation is further complicated by the requirement that the two-electron wave function be totally antisymmetric, with the symmetric triplet spinor paired with the antisymmetric-configuration space wave function, and the antisymmetric singlet spinor paired with the symmetric-configuration space wave function.

The spin-averaged triple-differential electron scattering cross section for electron impact ionization of atomic hydrogen can then be written as the statistically weighted sum of singlet and triplet cross sections. In terms of the direct and exchange scattering amplitudes, $f(\vec{k}_1', \vec{k}_2')$ and $g(k_1', k_2')$, respectively, the electron scattering cross section can be expressed as¹

$$\frac{d^3\bar{\sigma}}{d\Omega_1 d\Omega_2 dE_1'} = \frac{k_1' k_2'}{k_1} \left(\frac{1}{4} |f+g|^2 + \frac{3}{4} |f-g|^2 \right), \quad (1)$$

with $|f+g|^2$ corresponding to the singlet and $|f-g|^2$ to the triplet cross section. Here \vec{k}_1 , \vec{k}_1' , and \vec{k}_2' are, respectively, the momenta (in atomic units) of the incident, scattered, and ejected electrons, and E_1' is the energy of the scattering electron. Since f and g are complex quantities, three independent parameters are needed to describe the problem; for example, $|f|^2$, $|g|^2$, and $\text{Re}(f^*g)$. These separately calculable quantities can only be determined by polarization experiments. As an ancillary benefit, experiments with polarized particles remove the requirement of the absolute determination of beam fluxes, target densities, and detector efficiencies—quantities which are often difficult to measure with precision. In the case of electron impact ionization of atomic hydrogen, the imprecise knowledge of the ion-detection efficiency might account for the disagreement among the various experimental measurements.²

In this Letter we report on the first polarized-beams experiment involving the collision of polarized electrons with polarized hydrogen atoms.³

We measured the antiparallel-parallel asymmetry, A , in the ionization cross section given by

$$A = (\sigma^{\uparrow\downarrow} - \sigma^{\uparrow\uparrow}) / (\sigma^{\uparrow\downarrow} + \sigma^{\uparrow\uparrow}), \quad (2)$$

where the arrows indicate the antiparallel- and parallel-spin configurations. Partial (singlet or triplet, for example) ionization cross sections, σ_j , are obtained from the corresponding partial triple-differential electron scattering cross section $d^3\sigma_j/d\Omega_1 d\Omega_2 dE_1'$ according to¹

$$\sigma_j = \frac{1}{2} \int_0^E dE_1' \iint \frac{d^3\sigma_j}{d\Omega_1 d\Omega_2 dE_1'} d\hat{k}_1' d\hat{k}_2', \quad (3)$$

where $(E + \frac{1}{2})$ is the energy (in atomic units) of the incident electron.

For the purpose of theoretical comparison the asymmetry A can be re-expressed as the ratio

$$A = \sigma_{\text{int}} / \bar{\sigma}, \quad (4)$$

where σ_{int} is the interference cross section obtained from

$$\frac{d^3\sigma_{\text{int}}}{d\Omega_1 d\Omega_2 dE_1'} = \frac{k_1' k_2'}{k_1} \text{Re}[f^*(\vec{k}_1', \vec{k}_2') g(\vec{k}_1', \vec{k}_2')] \quad (5)$$

in accordance with Eq. (3), and $\bar{\sigma}$ is the total spin-averaged cross section. It can be shown⁴ that σ_{int} is also given by

$$\sigma_{\text{int}} = \sigma - \bar{\sigma}, \quad (6)$$

where σ is the total cross section calculated in the absence of exchange-symmetry considerations. Thus A can be deduced, for example, from Born calculations for σ and Born-exchange calculations^{1,4-7} for $\bar{\sigma}$. Alternatively, A can be written

as

$$A = (1 - r) / (1 + 3r), \quad (7)$$

where r is the ratio of the triplet to the singlet cross section.

The layout used in our experiment is illustrated schematically in Fig. 1. The polarized electron source, based upon the Fano effect in cesium,⁸ is described in detail elsewhere.⁹ Briefly, circularly polarized light of wavelength $280 \geq \lambda \geq 318$ nm ionizes an atomic beam of Cs in a region maintained at -1 -kV electrostatic potential. As a result of the spin-orbit interaction in the continuum state, the photoelectrons are highly spin polarized along the light axis. The photoelectrons are extracted from the ionization region by a potential gradient of ~ 1 V/cm and then accelerated to ground potential and formed into a beam by means of electron-optical focusing elements. Typically, the extracted beam current is 15 nA, and the energy spread (determined by filter lens cutoff measurements and by threshold behavior of hydrogen ionization) is 3.0 eV full width at half-maximum.

Light from a 1000-W Hg-Xe arc lamp is circularly polarized by a dichroic film polarizer and a zeroth-order quartz quarter-wave retardation plate. Rotation of either the polaroid or the quarter-wave plate by 90° reverses the electron polarization. The bending magnet shown in Fig. 1 can be adjusted to deflect the electron beam into either the interaction region or the Mott analyzer.¹⁰ In the Mott branch, the electron polarization is first rotated to a transverse orientation in a Wien filter and then accelerated to 100 keV

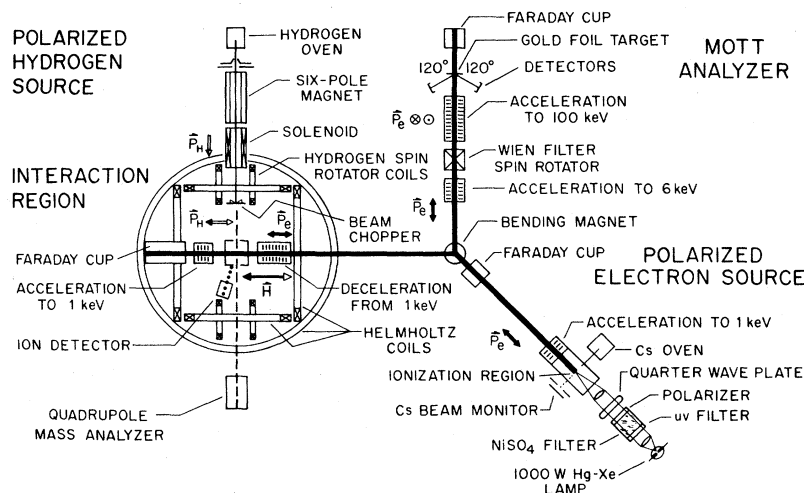


FIG. 1. Schematic diagram of the experimental layout.

for Mott analysis. Typically the electron polarization, P_e , is measured to be 0.63 ± 0.03 .⁹

The hydrogen source is a tungsten tube, resistively heated to ~ 2800 K, into which molecular hydrogen is bled. After collimation, the atomic $m_j = +\frac{1}{2}$ states of the partially dissociated beam are selected at high field in a six-pole magnet. A computer analysis, based upon an optical model of the focusing properties of the six-pole magnet,¹⁰ shows that the high-field state-selection parameter, s , of the atomic hydrogen reaching the interaction region is > 0.99 . Since the scattering experiment is carried out in a near-zero-field region, the hyperfine interaction in the ground state results in an electronic-spin polarization, P_H , of the atom given by $P_H = \frac{1}{2}s$.¹⁰

In order to minimize the possibility of Majorana depolarization of the hydrogen beam, the atoms emerging from the six-pole magnet are first aligned in a ~ 200 -G axial field of a small solenoid and then adiabatically rotated into an orientation parallel (or antiparallel) to the electron beam while within the ~ 5 -G field of a small Helmholtz pair. The atoms then experience a field which always remains parallel to the electron-beam axis as it monotonically decreases to a value of ~ 200 mG at the interaction region. Before entering the interaction chamber, the atomic beam is modulated by a 100-Hz tuning-fork beam chopper. After leaving the interaction chamber, the beam enters a final chamber containing a quadrupole mass analyzer which monitors the relative amounts of atomic and molecular hydrogen. In the interaction region the atomic hydrogen density is estimated to be $(1-2) \times 10^9$ atoms/cm³, while the residual gas pressure is $\sim 10^{-9}$ Torr.

Prior to entering the interaction region, the electron beam is decelerated to an energy of several eV and collimated. Then the beam is reaccelerated to the desired potential relative to the electron source, the absolute energy scale being established by the onset of ionization at 13.6 eV. After intersection with the hydrogen beam, the unscattered electrons are accelerated to ground potential into a Faraday cup.

The current arriving in the cup is digitized by an electrometer and voltage-to-frequency converter (VFC). The output of the VFC is counted in a preset scaler which halts data taking after a preset charge has arrived at the cup. For each data interval (5–10 sec) the ion counts detected by the bare multiplier shown in Fig. 1 are totaled on a pair of blind scalars according to whether

they occurred during the beam-on or beam-off portions of the chopper cycle. Likewise, the quadrupole signals for both H_1 and H_2 are totaled in pairs of blind scalars representing beam on and beam off. Also recorded for each data-taking interval is the accumulated charge in the Faraday cup and the elapsed time. At the completion of a data-taking interval, a PDP-15 computer reads and clears the blind scalars, advances the quarter-wave plate by 90° , and reinitiates data accumulation. After approximately twenty complete revolutions of the quarter-wave plate (10–15 min), the run is halted and the accumulated totals (typically 15 000 beam-on and 2500 beam-off events at 27 eV) for each quarter-wave-plate position are read onto magnetic tape. A complete measurement at a given energy normally comprises eight runs corresponding to four orientations of the linear polarizer 90° apart for each of the two directions of the magnetic field in the interaction region.

The asymmetry, Δ_R , for each run is defined as

$$\Delta_R = (N_+ - N_- - B_+ + B_-) / (N_+ + N_- - B_+ - B_-), \quad (8)$$

where N_+ is the sum of the beam-on ion counts for quarter-wave-plate positions 0 and 2 (0° and 180°), N_- is the sum of the beam-on ion counts for quarter-wave-plate positions 1 and 3 (90° and 270°), and B_+ and B_- are the corresponding sums of beam-off ion counts. In addition to the real asymmetry just defined, two false asymmetries, Δ_1 and Δ_2 , can be constructed by taking different combinations of quarter-wave-plate positions, $(0) + (1) - (2) - (3)$ and $(0) + (3) - (1) - (2)$, respectively. For both the real and false asymmetries, the values of Δ measured for each run are combined according to their statistical weights to give a final asymmetry for a given energy. The physical asymmetry, A , is related to Δ_R by $\Delta_R = P_e P_H (1 - F) A$, where P_e and P_H are the polarizations of the electron and hydrogen beams, respectively, and F is the fraction of ion counts originating from molecular hydrogen.

Measurement of F is accomplished by lowering the oven temperature to approximately 1000 K, where it is assumed that the beam is entirely molecular in composition. The observed beam-related counting rate $N - B$, divided by the beam-on-minus-beam-off quadrupole H_2 signal, indicates the sensitivity of the experiment to molecular hydrogen. The product of this ratio and the H_2 signal at full temperature gives the number of counts attributable to molecular hydrogen at full temperature. The value of F so determined var-

TABLE I. Results of data analysis.^a

E (eV)	Δ_1 (10^{-4})	Δ_2 (10^{-4})	$\chi^2(0)/\text{deg.}$ Δ_1	freedom Δ_2	A
15	-56(30)	13(30)	16/13	10/13	0.515(32)
17	15(20)	-15(20)	7/10	11/10	0.479(28)
19	-12(27)	-55(27)	5/10	15/10	0.472(35)
23	38(25)	17(25)	15/9	13/9	0.465(35)
27	3(5)	3(5)	71/68	67/68	0.415(20)
34	-00(22)	02(22)	3/5	3/5	0.343(33)
42	05(11)	18(11)	9/10	16/10	0.338(17)
57	-04(15)	01(15)	15/9	6/9	0.256(15)
77	-11(22)	13(22)	10/9	13/9	0.201(20)
107	27(13)	05(13)	21/12	5/12	0.147(11)
147	04(12)	08(12)	12/8	8/8	0.128(13)
197	-20(16)	-00(16)	8/8	7/8	0.074(17)

^aUncertainties are 1 standard deviation; those for A include systematic as well as statistical effects.

ies from a few percent near threshold to -20% at higher energies.

The measured values of A are given in Table I together with the two false asymmetries for each energy. The systematic uncertainties in A result from uncertainties in P_e ($\pm 4\%$), P_H ($\pm 2\%$), $1-F$ ($\pm 1\%$), and the collinearity of the magnetic field with the electron beam ($\pm 2\%$).

In Fig. 2 is shown a comparison of experimental results with values of A deduced from a number of theoretical calculations. For curves j and k, Eq. (7) was used to generate A; for all other curves, Eqs. (4) and (6) were used with the non-exchange results provided. It can be seen that none of the theoretical calculations is in good agreement with the experimental data, particularly at low energy. While the Born and Glauber calculations are not expected to be accurate at low energy, the substantial disagreement with the close-coupling results is more surprising. It should be noted that although the threshold value of $A = +1.0$, predicted by the recent work of Klar and Schlecht,¹³ cannot be confirmed by our measurements, A is still increasing with decreasing energy at 15 eV. It is clear that future polarization experiments in the threshold region would be very valuable. It is equally clear that more accurate theoretical calculations of electron impact ionization of hydrogen are needed at all energies.

We thank Dr. A. Temkin for calling our attention to the work of Klar and Schlecht. We also acknowledge contributions by Professor W. Raith

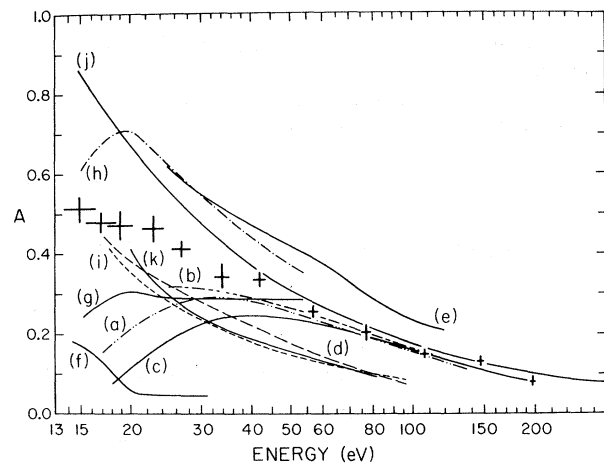


FIG. 2. Experimental values of A and theoretical predictions based upon Eqs. (6) and (7). Curves a, b, c, and d are Born-exchange (BE) calculations taken from Refs. 1, 4, 5, and 6, respectively. Curve e, taken from Ref. 4, is a BE calculation with maximum interference. Curve f, taken from Ref. 7, is also a BE calculation but with an angle-dependent potential. Curves g and h, both taken from Ref. 1, are spherical-average-exchange calculations, the latter allowing for maximum interference. Curves i, j, and k are, respectively, Glauber-exchange, modified Born-Oppenheimer, and close-coupling calculations taken from Refs. 6, 11, and 12.

and Dr. G. Baum, and the technical assistance of A. Disco. This research was supported in part by the National Science Foundation under Grant No. PHY76-84469 and by the U. S. Office of Naval Research under Contract No. N00014-76-C-0077.

¹See, for example, M. R. H. Rudge and M. J. Seaton, Proc. Roy. Soc. London, Ser. A, **283**, 262 (1965).

²W. L. Fite and R. T. Brackman, Phys. Rev. **112**, 1141 (1958); A. Boksenberg, thesis, University College, London, 1960 (unpublished); E. W. Rothe *et al.*, Phys. Rev. **125**, 582 (1962); J. W. McGowen and E. M. Clarke, Phys. Rev. **167**, 43 (1968).

³For preliminary results on elastic scattering see M. J. Alguard *et al.*, in Proceedings of the Tenth International Conference on the Physics of Electronic and Atomic Collisions, Paris, France, 21-27 July 1977 (to be published).

⁴R. K. Peterkop, Zh. Eksp. Teor. Fiz. **41**, 1938 (1961) [Sov. Phys. JETP **14**, 1377 (1962)].

⁵S. Geltman *et al.*, Proc. Phys. Soc., London **81**, 375 (1963).

⁶J. E. Goldin and J. H. McGuire, Phys. Rev. Lett. **32**, 1218 (1974).

⁷M. R. H. Rudge and S. B. Schwartz, Proc. Phys. Soc.,

London 88, 563 (1966).

⁸G. Baum *et al.*, Phys. Rev. A 5, 1073 (1972); U. Heinzmann *et al.*, Z. Phys. 240, 42 (1970).

⁹P. F. Wainwright *et al.*, to be published.

¹⁰See, for example, V. W. Hughes *et al.*, Phys. Rev.

A 5, 195 (1972).

¹¹V. I. Ochkur, Zh. Eksp. Teor. Fiz. 47, 1746 (1964) [Sov. Phys. JETP 20, 1175 (1965)].

¹²D. F. Gallaher, J. Phys. B 7, 362 (1974).

¹³H. Klar and W. Schlecht, J. Phys. B 9, 1699 (1976).

Upper-Hybrid-Resonance Absorption of Laser Radiation in a Magnetized Plasma

C. Grebogi, C. S. Liu, and V. K. Tripathi

Department of Physics and Astronomy, University of Maryland, College Park, Maryland 20742

(Received 19 May 1977; revised manuscript received 18 July 1977)

A magnetic field in a laser-irradiated plasma is shown to have an important effect on the resonant absorption of the laser radiation normally incident on the inhomogeneous plasma. For typical parameters in laser-fusion experiments, the absorption coefficient is above 50% with $\alpha \equiv \pi^2(\omega_c/\omega)^2(L\omega/c)^{4/3}$ between 1.5 and 10 and a maximum of $\sim 70\%$ is achieved for $\alpha=4$.

In laser-pellet fusion experiments, a magnetic field of a few megagauss is generated near the critical surface by a variety of sources such as $\nabla n \times \nabla T$, ponderomotive force, etc.¹⁻⁵ This self-generated magnetic field has been observed experimentally^{6,7} and in computer simulations. Because the magnetized plasma can support an upper hybrid wave, linear conversion of the laser radiation into this wave constitutes an anomalous absorption which has also been explored in numerical simulations.⁸ In this Letter we present an analytic theory of linear wave transformation whereby the normally incident laser radiation is converted into an upper hybrid wave at the resonance layer. Significant absorption with absorption coefficient $\geq 10\%$ is attained for the parameter $\alpha = \pi^2(\omega_c/\omega)^2(L\omega/c)^{4/3}$ in the range $0.2 < \alpha < 75$. Here α/π^2 is the square of the ratio of the distance between the cutoff and the resonance layers $x_0 = L\omega_c/\omega$ and the scale of variation of the electromagnetic wave near the cutoff $x_{em} = (Lc^2/\omega^2)^{1/3}$, L is the density scale length, $\omega_c = eB/mc$, and ω is the laser frequency. Absorption of 67% is achieved for $\alpha=4$ and a broad maximum ($>50\%$) absorption coefficient is found for typical parameters in laser-fusion experiments, i.e., $1.5 \lesssim \alpha \lesssim 10$.

It is well known that whenever an electromagnetic wave has a singularity near the point where the dielectric function for electrostatic waves vanishes, the electromagnetic wave can be converted into an electrostatic wave and anomalous absorption of the electromagnetic wave energy takes place with the generation of large-amplitude electrostatic waves. In an unmagnetized, inhomogeneous plasma, an obliquely incident electro-

magnetic wave with polarization in the plane of incidence can drive a density oscillation, because of the component of the electric field along the density gradient, giving rise to a nonvanishing $\nabla \cdot (n\vec{v}_{os})$, where $\vec{v}_{os} = -e\vec{E}_0/im\omega + c.c.$ At the critical density, where $\omega_p(x) = \omega$, $\omega_p = (4\pi ne^2/m)^{1/2}$, the plasma wave is resonantly driven by the electromagnetic wave tunneling through the reflection point (cutoff).⁹⁻¹² Piliya⁹ has given a very elegant analysis of this process. Because of the self-generated magnetic field in laser-produced plasmas, two new features are introduced into this process of resonant absorption. First, the resonant frequency is now the upper hybrid frequency $\omega_{uh} = (\omega_p^2 + \omega_c^2)^{1/2}$, instead of the plasma frequency ω_p ; second, the Lorentz force provides coupling between the electromagnetic and electrostatic waves so that, even for normal incidence, mode conversion into an upper hybrid wave takes place and significant absorption of the incident laser energy results. This upper-hybrid-wave conversion has been experimentally studied by Dreicer.¹³

In the present Letter we have investigated the wave conversion of an extraordinary mode in a magnetoplasma around the point of upper hybrid resonance taking thermal effects into account. For the sake of mathematical convenience, the direction of wave propagation is taken along the density gradient, perpendicular to the magnetic field. This well-known problem was first studied theoretically by Budden¹⁴ and recently re-examined by White and Chen,¹⁵ both using the cold-plasma approximation. To render the electromagnetic wave equation in the form of a Whittaker equation, they chose a very specific density pro-